

EVALUATION OF THE CONFORMATIONAL, HYDROGEN BONDING AND CRYSTAL PACKING PREFERENCES OF ACYCLIC IMIDES

SUSAN M. REUTZEL* AND MARGARET C. ETTER†

Department of Chemistry, University of Minnesota, Minneapolis, Minnesota 55455, U.S.A.

The molecular recognition properties of 18 acyclic imides were studied to evaluate the relative contributions of conformational, hydrogen bonding and crystal packing forces to the stabilization of specific aggregate patterns in the solid state. The crystal structure of diisobutyramide and the aggregate patterns of the 18 imides are presented. The stabilization by hydrogen bonding was found to override the conformational preferences of imides, while packing forces often precluded the formation of the most stable hydrogen bonded aggregate. The aggregate patterns of imides were also found to be a function of the type of substituents present as R groups. Imides with R groups of similar shape and size prefer to pack as bifurcated hydrogen bonded chains, whereas dimers or singly hydrogen-bonded chains form when the R groups have significantly different spatial requirements. Analysis of imide aggregate patterns revealed the similar spatial requirements of isopropyl and phenyl groups. The molecular recognition properties of acyclic imides are summarized as a set of hydrogen bond rules, which can be used to design new imide aggregates.

INTRODUCTION

Small molecules have been used extensively to model the specific binding interactions found in larger biochemical systems. Much effort has been put into designing synthetic receptors, which are relatively rigid and have complementary hydrogen bonding functionality in appropriately sized cavities, to bind biologically significant molecules.¹ Rigidity has been found to enhance binding, partly because it keeps the host from self-associating.² Flexible host–guest systems have been particularly useful in studying the selectivity of self-assembly by hydrogen bonding, yet in these systems self-association often competes with complexation. Therefore, to understand the origin of the specific competitive hydrogen bonding processes that occur in flexible host–guest systems, the molecular recognition properties of the individual host and guest molecules must also be considered.

As part of a comprehensive study of the molecular recognition properties of small organic molecules,³ we have recently reported studies on the host–guest chemistry of acyclic imides using co-crystallization as a synthetic tool for preparing host–guest complexes.⁴ In this paper, we focus on the properties of the host alone.

We find that the hydrogen bond properties that host molecules exhibit in the presence of guest molecules can often be derived from the way the host molecules bind to themselves in their own homomeric crystal forms. The factors contributing to the observed hydrogen bonding patterns include conformational energy profiles and differential steric demands and hydrogen bond strengths. In this paper, we show that several common features recur in 20 acyclic imide aggregate patterns, including that of diisobutyramide (5), whose crystal structure is presented here, and report that it is often possible to predict *a priori* which pattern is expected for a particular imide.

EXPERIMENTAL

General methods. Melting points were determined on a Fischer–Johns apparatus and are uncorrected. Infrared spectra were recorded on a Nicolet 5DXB Fourier transform spectrometer from Nujol mulls and are reported in cm^{-1} . ^1H and ^{13}C NMR spectra were recorded on IBM NR200AF and Varian VXR-300 spectrometers, respectively, and chemical shifts are reported in parts per million (δ) from tetramethylsilane. ^{13}C

* Present address: Eli Lilly and Company, Indianapolis, IN 46285, U.S.A.

† Author to whom correspondence should be addressed.

cross-polarization magic angle spinning (CP-MAS) NMR spectra were recorded on an IBM NR100AF spectrometer operating at a carbon frequency of 25.178 MHz and with a Doty solid-state probe. ^{13}C chemical shifts are reported (δ) relative to *p*-di-*tert*-butylbenzene (CH_3 δ 31.0). Spectroscopic-grade solvents were used for all recrystallizations. Deuterated solvents were obtained from Aldrich Chemical. Acyclic imides, **1**, **10–12** and **15–18**, were synthesized and their hydrogen bonding patterns characterized in the solid state as described previously.^{4,5}

N-Acetylpropionamide (2). To a stirred solution of 5.0 g (68 mmol) of propionamide in 25 ml of CCl_4 were added 0.1 ml of concentrated H_2SO_4 and 4.8 ml (68 mmol) of acetyl chloride in 5 ml of CCl_4 dropwise by syringe over 1 h. After refluxing for 10 h, the solvent was removed *in vacuo*. Recrystallization from diethyl ether afforded **2** (quantitative yield) as colorless plates: m.p. 85–86 °C (lit.^{6a} m.p. 86–87 °C); IR (Nujol), 3271, 3178, 1761, 1732, 1539, 1506, 1419, 1243, 1178, 1080, 1036, 995, 938, 879, 808 and 735 cm^{-1} ; ^1H NMR (200 MHz, CDCl_3), δ 1.13 (t, 3 H, $J = 7.3$ Hz), 2.33 (s, 3 H), 2.55 (q, 2 H, $J = 7.4$ Hz) and 9.31 (bs, 1 H); ^{13}C NMR (50 MHz, CDCl_3), δ 8.4, 25.0, 30.6, 171.3 and 173.9; ^{13}C CP-MAS NMR (25 MHz), δ 7.5, 24.2, 30.2, 169.2, 172.7, 176.6 and 178.6.

Dipropionamide (3). Dipropionamide was obtained by acid-catalyzed condensation of propionamide and propionyl chloride.^{6b} Recrystallization from ethanol gave colorless plates: m.p. 154–156 °C (lit.^{6b} m.p. 154 °C); IR (Nujol), 3177, 3268, 1736, 1507, 1422, 1366, 1186, 1073 and 723 cm^{-1} ; ^1H NMR [200 MHz, $(\text{CD}_3)_2\text{CO}$], δ 1.06 (t, 3 H, $J = 7.4$ Hz), 2.58 (q, 2 H, $J = 7.4$ Hz) and 9.4 (bs, 1 H); ^{13}C NMR (50 MHz, CDCl_3), δ 8.4, 30.7 and 174.2; ^{13}C CP-MAS NMR (25 MHz), δ 6.9, 29.9, 171.9 and 179.0.

Di-n-butyramide (4). To a stirred solution of 2.5 g (27 mmol) of *n*-butyramide in 25 ml of CCl_4 were added 0.1 ml of concentrated H_2SO_4 and 2.98 ml (27 mmol) of *n*-butyryl chloride in 5 ml of CCl_4 . The mixture was refluxed for 6 h, then the solvent was removed *in vacuo*. Recrystallization from light petroleum yielded 1.2 g of pure **4** as a white solid (28% yield): m.p. 80–82 °C; IR (Nujol), 3262, 3177, 1733, 1503, 1464, 1414, 1341, 1307, 1272, 1169, 1076 and 724 cm^{-1} ; ^1H NMR (200 MHz, CDCl_3), δ 0.97 (t, 3 H, $J = 7.4$ Hz), 1.67 (sext, 2 H, $J = 7.4$ and 7.5 Hz), 2.56 (t, 2 H, $J = 7.3$ Hz) and 8.28 (bs, 1 H); ^{13}C NMR (50 MHz, CDCl_3), δ 13.9, 18.0, 39.5 and 173.4; ^{13}C CP-MAS NMR (25 MHz), δ 13.5, 16.0, 37.5, 170.8 and 175.8.

Diisobutyramide (5). To a stirred solution of 2.0 g (23 mmol) of isobutyramide in 10 ml of freshly distilled

THF (sodium spheres–benzil ketyl) at 0 °C were added 9.2 ml (23 mmol) of 2.5 M *n*-butyllithium in hexane dropwise by syringe. The suspension was stirred for 10 min and cooled to –78 °C. After stirring for an additional 10 min, 2.4 ml (23 mmol) of isobutyryl chloride were added dropwise by syringe. The solution was stirred for 10 min and then allowed to warm to room temperature, at which time 10 ml of saturated NH_4Cl were added. The white solid was filtered, dissolved in hot water and extracted with EtOAc. The organic extracts were combined and the solvent was removed *in vacuo* to yield **5** (1.4 g, 38%); m.p. 153–155 °C; IR (Nujol), 3263, 3181, 1732, 1521, 1507, 1463, 1383, 1181, 1169, 1107 and 721 cm^{-1} ; ^1H NMR [200 MHz, $(\text{CD}_3)_2\text{SO}$], δ 1.03 (d, 12 H, $J = 6.8$ Hz), 2.88 (sept, 2 H, $J = 6.8$ Hz) and 10.4 (bs, 1 H); ^{13}C NMR (50 MHz, $(\text{CD}_3)_2\text{SO}$), δ 18.9, 34.6 and 177.5; ^{13}C CP-MAS NMR (25 MHz), δ 16.5, 20.1, 35.0, 175.7, and 182.6.

N-Acetylisobutyramide (6). To a stirred solution of 1 g (11.5 mmol) of isobutyramide in 50 ml of toluene were added 0.1 ml of concentrated H_2SO_4 and 0.82 ml (11.5 mmol) of acetyl chloride in 5 ml of toluene. The mixture was refluxed for 24 h then the solvent was removed *in vacuo* to yield 0.8 g of pure **6** as a white solid (52% yield): m.p. 56–58 °C; IR (Nujol), 3276, 3177, 1733, 1697, 1516, 1466, 1376, 1243, 1188, 1156, 1108, 1023, 918 and 730 cm^{-1} ; ^1H NMR (200 MHz, CDCl_3), δ 1.16 (d, 6 H, $J = 6.9$ Hz), 2.42 (s, 3 H), 2.67 (sept, 1 H, $J = 6.8$ Hz), and 8.4 (bs, 1 H); ^{13}C NMR (50 MHz, CDCl_3), δ 18.8, 25.3, 35.9, 172.4 and 176.1; ^{13}C CP-MAS NMR (25 MHz), δ 17.6, 23.8, 35.0, 168.7, 175.1 and 181.2.

N-(Cyclohexylcarbonyl)cyclohexylamide (7). To a stirred solution of 3 g (24 mmol) of cyclohexanecarboxamide in 30 ml of freshly distilled THF (sodium spheres–benzil ketyl) at 0 °C were added 9.4 ml (24 mmol) of 2.5 M *n*-butyllithium in hexane dropwise by syringe. The solution was stirred for 10 min and cooled to –78 °C. After stirring for an additional 10 min, 3.2 ml (24 mmol) of cyclohexanecarbonyl chloride were added dropwise by syringe. The solution was stirred for 30 min and then allowed to warm to room temperature, at which time 5 ml of saturated NH_4Cl solution were added. The white solid was filtered, dissolved in hot water and extracted with EtOAc. The organic extracts were combined and the solvent was removed *in vacuo* to yield **7** (4.0 g, 71%); m.p. 190–192 °C IR (Nujol), 3262, 3170, 1732, 1695, 1525, 1507, 1464, 1454, 1315, 1244, 1171, 1161 and 1138 cm^{-1} ; ^1H NMR [200 MHz, $(\text{CD}_3)_2\text{CO}$], δ 1.26–1.36 (m, 10 H), 1.5–2.5 (m, 10 H), 2.8–3.0 (m, 2 H) and 9.5 (bs, 1 H); ^{13}C NMR [50 MHz, $(\text{CD}_3)_2\text{SO}$], δ 25.3, 25.5, 28.7, 44.3 and 176.4; ^{13}C CP-MAS NMR (25 MHz), δ 26.5, 45.1, 174.2 and 180.7.

N-(Phenylacetyl)phenylacetamide (8). To a stirred solution of 1.5 g (11 mmol) of phenylacetamide and 0.1 ml of concentrated H_2SO_4 in 20 ml of toluene were added 1.5 ml (11 mmol) of phenylacetyl chloride in 5 ml of toluene dropwise by syringe over 30 min. After the solution had been refluxed for 6 h, the solvent was removed *in vacuo*. The solid which remained was washed with EtOAc and dried to yield **8** (0.97 g, 36%) as a pale yellow solid: m.p. 193–195 °C; IR (Nujol), 3262, 3170, 1729, 1526, 1496, 1456, 1419, 1346, 1319, 1226, 1139, 726, 697 and 690 cm^{-1} ; ^1H NMR [$(\text{CD}_3)_2\text{SO}$], δ 3.86 (s, 4 H), 7.29 (m, 10 H) and H(N) not found; ^{13}C NMR [50 MHz, $(\text{CD}_3)_2\text{SO}$], δ 43.3, 126.8, 128.4, 129.7, 134.8 and 171.9; ^{13}C CP-MAS NMR (25 MHz), δ 42.4, 125.7, 127.6, 130.6, 135.3, 170.0, and 176.1.

Dipivalamide (9). To a stirred suspension of pivalamide (2 g, 19.8 mmol) in 20 ml of freshly distilled THF at 0 °C were added 7.9 ml of 2.5 M *n*-butyllithium (19.8 mmol) by syringe. The solution was stirred at 0 °C for 10 min and cooled to –78 °C, then 2.4 ml of pivaloyl chloride (19.8 mmol) were added dropwise by syringe. The mixture was stirred for 10 min, warmed to 0 °C and quenched with saturated ammonium chloride. The white solid was collected by filtration and purified by flash chromatography (5% ethyl acetate–hexane) to afford **9**: m.p. 107–110 °C (lit.⁴ m.p. 109 °C); IR (Nujol), 3408, 3382, 1750, 1460, 1401, 1377, 1132 and 1111 cm^{-1} ; ^1H NMR [200 MHz, $(\text{CD}_3)_2\text{SO}$] δ 1.19 (s, 18 H) and 8.96 (bs, 1 H); ^{13}C NMR [50 MHz, $(\text{CD}_3)_2\text{SO}$] δ 26.6, 40.4 and 176.0; ^{13}C CP-MAS NMR (25 MHz), δ 27.6, 40.9, 174.0 and 179.8.

N-Isobutyrylbenzamide (13). To a stirred solution of 5 g (41 mmol) of benzamide in 20 ml of hot acetonitrile were added 4.3 ml (41 mmol) of isobutyryl chloride in 5 ml of acetonitrile dropwise. After the solution had been refluxed for 2 h, it was poured over 100 ml of ice and warmed to room temperature. The solid was filtered, washed with 5% NaHCO_3 and recrystallized from methanol–water to yield **13** (3.2 g, 40%) as a white crystalline solid: m.p. 156–157 °C (lit.⁴ m.p. 156 °C); IR (Nujol), 3267, 3157, 3062, 1749, 1722, 1683, 1673, 1601, 1581, 1505, 1488, 1465, 1385, 1273, 1182, 1153, 1105, 708 and 688 cm^{-1} ; ^1H NMR (200 MHz, CDCl_3) δ 1.25 (d, 6 H, $J = 6.8$ Hz), 3.65 (sept, 1 H, $J = 6.8$ Hz), 7.46–7.64 (m, 3 H, $J = 7.6$ Hz), 7.84 (d, 2 H, $J = 6.8$ Hz) and 8.5 (bs, 1 H); ^{13}C NMR [50 MHz, $(\text{CD}_3)_2\text{SO}$], δ 19.0, 34.8, 128.5, 132.7, 133.9, 166.6 and 178.0; ^{13}C CP-MAS NMR (25 MHz), δ 16.5, 20.6, 35.3, 127.6, 129.1, 132.0, 134.0, 165.5, 172.2, 177.7 and 184.2.

N-Pivaloylbenzamide (14). To a stirred suspension of benzamide (3 g, 24.8 mmol) in 20 ml of freshly dis-

tilled THF at 0 °C were added 9.9 ml of 2.5 M *n*-butyllithium (24.8 mmol) by syringe. The solution was stirred at 0 °C for 10 min and cooled to –78 °C, then 3.1 ml of pivaloyl chloride (24.8 mmol) were added dropwise by syringe. The mixture was stirred for 10 min, warmed to 0 °C and quenched with saturated ammonium chloride. The solid precipitate was collected by vacuum filtration, washed and dried to yield 1.6 g (32% yield) of **14**: m.p. 124–126 °C; IR (Nujol), 3311, 1733, 1685, 1507, 1480, 1447, 1258, 1133, 699, 669 and 630 cm^{-1} ; ^1H NMR (200 MHz, CDCl_3), δ 1.33 (s, 9 H), 7.44–7.58 (m, 3 H, J values include 5.7, 5.8, 6.9 and 1.7 Hz), 7.74 (d, 2 H, $J = 6.7$ and 1.7 Hz) and 8.5 (bs, 1 H); ^{13}C NMR (50 MHz, CDCl_3), δ 27.1, 40.6, 127.8, 128.8, 132.8, 133.9, 166.5 and 176.3; ^{13}C CP-MAS NMR (25 MHz), δ 25.9, 40.2, 128.0, 131.1, 136.1, 165.6, 173.0, 174.5 and 181.5.

Polymorphism. Polymorphs of acyclic imides were identified using powder x-ray diffraction (XRD), solid-state IR, melting point analysis, optical microscopy and ^{13}C CP-MAS NMR. Single crystals were isolated when possible and characterized by their different melting points and solid-state IR spectra. Bulk powder samples having melting points and IR spectra identical with those of the single crystal forms were then analyzed using XRD and ^{13}C NMR. XRD was also used to show that the samples were homogeneous.

Crystal structure determination for 5.⁷ Data were collected on an Enraf-Nonius CAD4 diffractometer with graphite monochromated $\text{Mo K}\alpha$ radiation ($\lambda = 0.71069$) using the ω – 2θ scan technique. Lattice parameters were obtained from least-squares analysis of 25 reflections. Structure was solved by direct methods with MITHRIL⁸ and DIRDIF.⁹ All non-hydrogen atoms were refined anisotropically. All NH protons were refined isotropically. The other hydrogen atoms included in the structure factor calculations were placed in idealized positions ($d_{\text{C-H}} = 0.95$ Å) with assigned isotropic thermal parameters ($B = 1.2B$ of bonded atoms). The experimental details of the x-ray analysis of **5** are given in Table 1. The last entry in Table 1 gives the graph set, which is a representation of the topology of hydrogen-bonded sets of molecules in the crystal.* A description of how this assignment was made and of how to use graph sets to analyze acyclic imide patterns will be given in a future paper.

* The notation used in graph set analysis is $G_d^a(r)$. The pattern designator, G , is assigned as S = intramolecular (or self), D = a non-cyclic finite pattern (e.g. a dimer), R = a cyclic finite pattern (ring) or C = an infinite pattern (chain). The parameters a and d refer to the number of acceptors and donors participating in the hydrogen bond, respectively. The degree or 'size' of the pattern, r , is given in parentheses. For a detailed discussion of graph set analysis, see Ref. 10.

Table 1. Crystallographic data for 5

Formula	C ₈ H ₁₅ NO ₂	μ (Mo K, α) (cm ⁻¹)	0.72
fw	157.21	T (°C)	23(1)
Space group	Iba2	No. of unique data, total	1122
a (Å)	8.992 (2)	No. of data used	828
b (Å)	12.139 (2)	R^a	0.034
c (Å)	8.876 (3)	R_w^b	0.042
α (°)	90.0	$2\theta_{\max}$ (°)	53.9
β (°)	90.0	Range of hkl	$0 \leq h \leq 11$
γ (°)	90.0		$-15 \leq k \leq 15$
V (Å ³)	968.8 (7)		$-10 \leq l \leq 11$
Z	4	(Shift/error) _{max}	0.44
d_{calc} (g·cm ⁻³)	1.08	Largest peak (e ⁻ Å ⁻³)	0.10
Crystal size (mm)	0.50 × 0.40 × 0.30	Graph set	C ₁ ² (4)[R ₁ ² (6)]

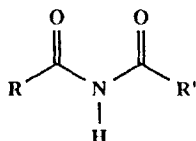
$$^a R = \Sigma ||F_0| - |F_c|| / \Sigma |F_0|$$

$$^b R_w = [(\Sigma w(|F_0| - |F_c|)^2) / \Sigma w F_0^2]^{1/2}; w = 4 F_0^2 / \sigma^2(F_0^2)$$

Molecular modelling. The energy minima of the possible planar *cis-cis*, *cis-trans* and *trans-trans* conformers of the arylalkyl imides were calculated with Macromodel,¹¹ a molecular mechanics program using the AMBER¹² force field.

RESULTS

The detailed patterns of hydrogen bonding and the forces contributing to these patterns were studied for a series of acyclic imides. Fifteen acyclic imides, 1–15, having no hydrogen-bonding functional groups other

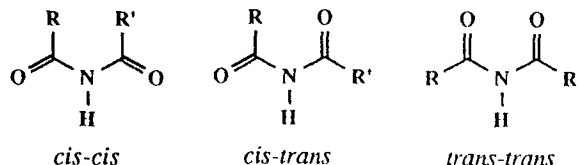


Imide	R	R'
1	—CH ₃	—CH ₃
2	—CH ₃	—CH ₂ CH ₃
3	—CH ₂ CH ₃	—CH ₂ CH ₃
4	—CH ₂ CH ₂ CH ₃	—CH ₂ CH ₂ CH ₃
5	—CH(CH ₃) ₂	—CH(CH ₃) ₂
6	—CH ₃	—CH(CH ₃) ₂
7	—CH(CH ₂) ₅	—CH(CH ₂) ₅
8	—CH ₂ Ph	—CH ₂ Ph
9	—C(CH ₃) ₃	—C(CH ₃) ₃
10	—CH ₃	—Ph
11	—CH ₂ CH ₃	—Ph
12	—CH ₂ CH ₂ CH ₃	—Ph
13	—CH(CH ₃) ₂	—Ph
14	—C(CH ₃) ₃	—Ph
15	—Ph	—Ph
16	—CH ₃	—(2—OH)Ph
17	—CH ₂ CH ₃	—(2—OH)Ph
18	—Ph	—(2—OH)Ph

than —CONHCO—, and three having an additional hydroxyl group (16–18) were synthesized and their hydrogen bonding patterns characterized (details of the spectroscopic characterization will be given elsewhere¹³). Herein is presented the crystal structure of 5. The hydrogen bonding patterns of all 18 imides are also presented and interpreted in terms of conformational and hydrogen bonding preferences and solid-state packing efficiency.

Crystallographic studies of acyclic imides

Acyclic imides may exist in three planar conformations, *cis-cis*, *cis-trans* and *trans-trans*, differentiated by the relative positions of the carbonyl groups with respect to the central NH bond. Previously reported x-ray crystal structures of acyclic imides (uncomplexed and with no hydrogen bonding functional groups present in the R groups) show that the *trans-trans* conformation is found in six (1β, 3, 9, 10β, 13 and 15) of the nine known structures.^{5a,14,15} The other three imides, 1α, 11 and 12, adopt the *cis-trans* conformation in the solid state.



The x-ray crystal structure of 5 was determined to provide an insight into the role that substituents play in determining the molecular conformation and the hydrogen bonding and packing patterns of this class of compounds. Diisobutyramide, 5, is a sterically hindered dialkyl imide and is found in the *trans-trans* conformation in the solid state [Figure 1(a)].

Deviations of the —CONHCO— moiety from planarity due to repulsive 1,5 interactions between the

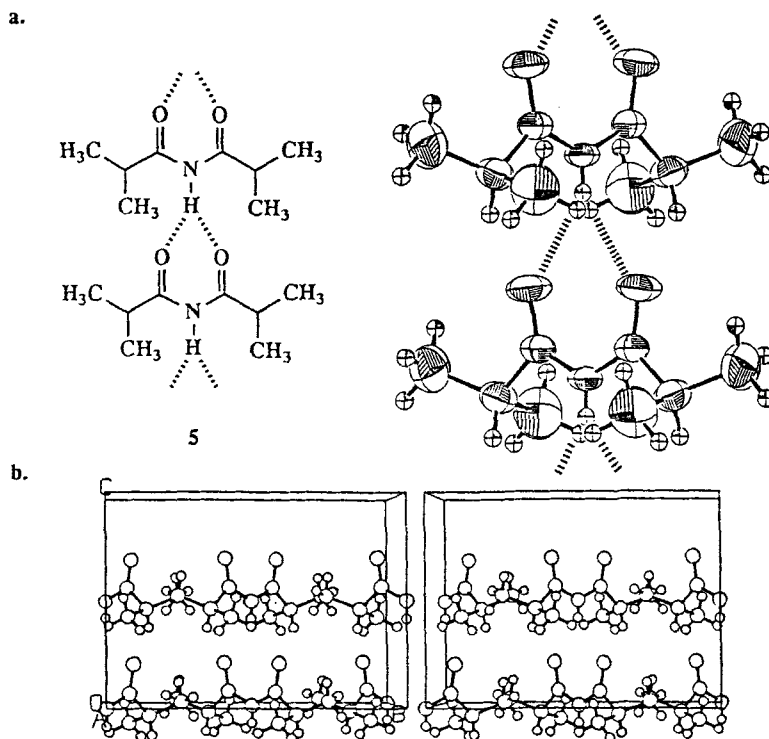


Figure 1. (a) Molecular geometry and hydrogen bond scheme of **5**. Molecules of **5** are observed in the *trans-trans* conformation and are hydrogen bonded in chains linked by bifurcated $\text{NH}\cdots\text{O}$ hydrogen bonds between screw-related molecules. In this structure, the hydrogen bond chains are oriented parallel to one another. Thermal ellipsoids are depicted at 50% probability. Dashed lines indicate hydrogen bonds. (b) Stereoscopic view of the unit cell of **5**, viewed along $[100]$

two oxygen atoms are seen in **5**. These distortions lead to an increase in the $\text{O}\cdots\text{O}$ separation in **5** from an ideal distance of about 2.4 Å, assuming normal bond lengths and 120° bond angles, to 2.758 (3) Å.

All imides have two potential hydrogen bond acceptors ($\text{C}=\text{O}$) and one hydrogen bond donor (NH), which are used in different ways in the three different hydrogen bonding patterns observed previously for nine known acyclic imides. The *cis-trans* conformers always

occur in a dimeric hydrogen bond pattern (hereafter called aggregate A) and all *trans-trans* conformers, except **9**, occur in chains. Usually the molecules in the chains are linked by bifurcated hydrogen bonds (aggregate B), but one structure (**10β**) has been found having the *trans-trans* imide linked into chains by two-centered hydrogen bonds (aggregate C). In aggregates A and C, only one of the hydrogen bond acceptors is used in forming hydrogen-bonded dimers and chains,

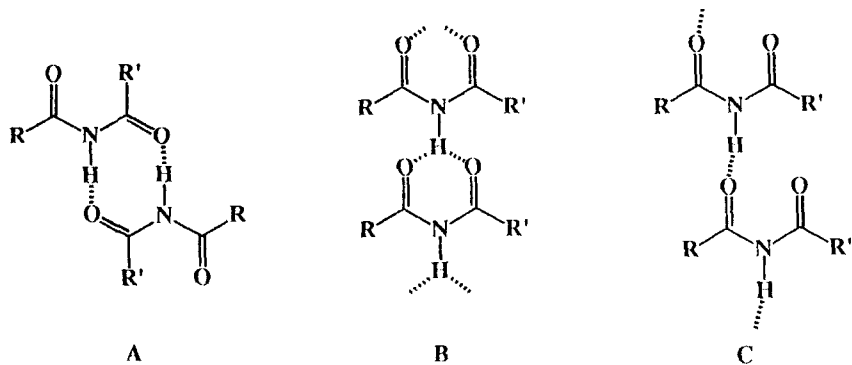
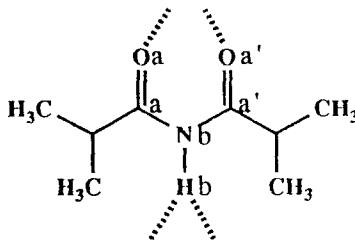


Table 2. Hydrogen bond geometries and selected intra- and intermolecular bond lengths for **5**


$C_a=O_a(\text{\AA})$	1.209(2)	$N_b\cdots O_a(\text{\AA})$	2.980(2)
$C_a-N_b-C_{a'}(^{\circ})$	128.1(2)	$H_b\cdots O_a(\text{\AA})$	2.34(3)
$N_b-C_a-O_a(^{\circ})$	122.7(2)	$N_b-H_b\cdots O_a(^{\circ})$	143.93

respectively. The *trans-trans* conformers in aggregate B use both hydrogen bond acceptors in forming chains linked by bifurcated $NH\cdots O$ hydrogen bonds, interactions which stabilize the *trans-trans* conformation in the solid state.¹²

The expected hydrogen bonding pattern for *trans-trans* imides, B, is observed in **5** [Figure 1(a)]. The bifurcated hydrogen-bonded chains are linked by $NH\cdots O$ hydrogen bonds from the NH of one molecule to the carbonyl groups of its neighbor [$NH\cdots O = 2.34(3) \text{ \AA}$, $N(H)\cdots O = 2.980(2) \text{ \AA}$] and are oriented along the *c* axis. The hydrogen bond geometries and selected intra and intermolecular bond lengths found in the structure of **5** are given in Table 2.

The unit cell packing pattern of **5** is shown in Figure 1(b). The mean molecular plane of one imide makes a dihedral angle of about 75° with screw-related molecules in the hydrogen bond chain. These hydrogen bond chains in **5** are all oriented in the same direction.

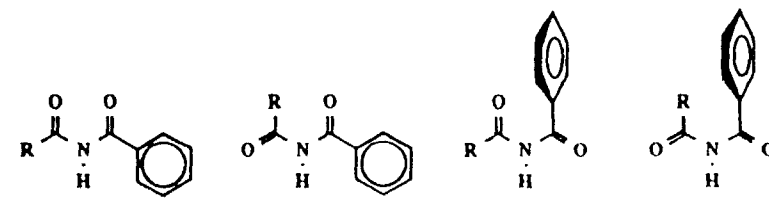
Comparative molecular conformations and hydrogen bond patterns of acyclic imides

Imides **2**, **4**, **6–8**, **10 α** and **14** were also synthesized and their hydrogen bonding patterns characterized by non-crystallographic means using solid-state IR and solution and solid-state ^{13}C NMR.⁵ Assignments of their hydrogen bond aggregates were made by extending correlations previously made between the spectral data of imides **1**, **3**, **5**, **9**, **10 β** , **11–13** and **15**, and specific structural features observed in their x-ray crystal structures.

By solid-state IR, imides **2**, **4**, **6–8** and **14** were found to be in the *trans-trans* conformation, whereas **10 α** was *cis-trans*, with the acetyl carbonyl *cis* and the benzoyl carbonyl *trans*. This *cis-trans* imide conformation is also observed in the other arylalkyl imides (**11** and **12**), where the alkyl group is primary. Both the *trans-trans* and the *cis-trans* conformations are observed in two separate polymorphs of **10** (α and β), but only one polymorph of **11** or **12** has yet been isolated.

We modelled the four possible planar imide conformers of **10–13** and **15** and determined their energies using Macromodel. The results of the energy minimizations are shown in Table 3. As expected, the *cis-trans* conformers observed in the solid state (column 4, Table 3) were found to be the most stable in **10–12**. The energy difference between the most stable *cis-trans* form and *trans-trans* form is smaller in **10** than it is in **11** or **12**, however ($0.12 \text{ kcal mol}^{-1}$ in **10** vs $0.29 \text{ kcal mol}^{-1}$ in **11** and **12**). This finding suggests that **10 α** and $-\beta$ are relatively close in energy so that either conformation is possible in the solid state. It is not clear that a $0.29 \text{ kcal mol}^{-1}$ energy difference should be consistent with polymorph formation, but to date none have been found for **11** and **12**.

Bulkier substituents (secondary, tertiary, phenyl) force the arylalkyl imides (**13–15**) into the *trans-trans*

Table 3. Conformational energies (kcal mol^{-1}) of arylalkyl imides^a


Imide	R	<i>t-t</i>	<i>c-t</i>	<i>t-c</i>	<i>c-c</i>
10	Me	2.02	1.90	4.44	8.42
11	Et	3.39	3.10	5.73	9.61
12	ⁿ Pr	4.00	3.71	6.36	10.13
13	ⁱ Pr	4.08	5.55	6.41	12.33
15	Ph	11.58	13.12	13.12	16.84

^a Energies calculated using Macromodel (AMBER force field).

Table 4. Acyclic imide hydrogen-bond patterns

Imide	R	R'	Solid-state aggregate
1 α, β	—CH ₃	—CH ₃	A, B
2	—CH ₃	—CH ₂ CH ₃	B ^a
3	—CH ₂ CH ₃	—CH ₂ CH ₃	B
4	—CH ₂ CH ₂ CH ₃	—CH ₂ CH ₂ CH ₃	B ^a
5	—CH(CH ₃) ₂	—CH(CH ₃) ₂	B
6	—CH(CH ₃) ₂	—CH ₃	C ^a
7	—CH(CH ₂) ₅	—CH(CH ₂) ₅	B ^a
8	—CH ₂ Ph	—CH ₂ Ph	B ^a
9	—C(CH ₃) ₃	—C(CH ₃) ₃	b
10 α, β	—Ph	—CH ₃	A ^a , C
11	—Ph	—CH ₂ CH ₃	A
12	—Ph	—CH ₂ CH ₂ CH ₃	A
13	—Ph	—CH(CH ₃) ₂	B
14	—Ph	—C(CH ₃) ₃	B ^a
15	—Ph	—Ph	B
16	—(2—OH)Ph	—CH ₃	c
17	—(2—OH)Ph	—CH ₂ CH ₃	c
18	—(2—OH)Ph	—Ph	c

^a Proposed hydrogen bond aggregate.^b Does not form hydrogen bonds in the solid state.^c Is involved in a different hydrogen bond aggregate.

conformation to avoid the destabilizing 1,5 steric interactions between the alkyl groups and their neighboring benzoyl oxygens. Macromodel also showed that the *trans-trans* forms of **13** and **15**, which are observed in the solid state, are their lowest energy conformers (Table 3).

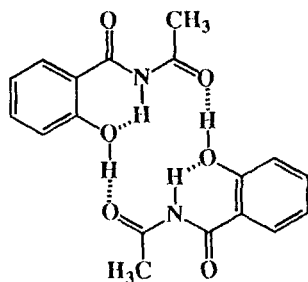
Hydrogen bonding interactions were characterized using solution and solid-state NMR. The NMR studies, coupled with the IR results, showed that the expected eight-membered ring dimer (aggregate A) is formed in **10 α** . Imides **2**, **4**, **7**, **8** and **14** were found to form B-type aggregates and **6** to form the relatively rare C-type aggregate. In this aggregate, the isobutyryl carbonyl group of **6** participates in hydrogen bonding and the acetyl carbonyl group is free. Table 4 summarizes the hydrogen bonding patterns observed for imides **1–18**.

So far we have focused on acyclic imide analogs that do not have any hydrogen bonding functionality other than the imide moiety itself. Intramolecular interactions with competitive functional groups can interfere with the inherent selectivity of the imide group as it forms intermolecular hydrogen bonds. Examples of how imide hydrogen bonding preferences are changed by introducing intramolecular hydrogen bonding functional groups are provided in the crystal structures of three salicylamide derivatives **16–18**.^{5b,16}

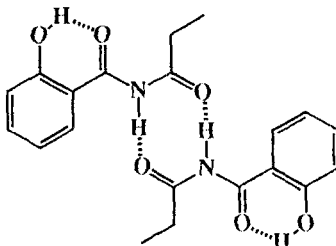
Interestingly, the molecular conformations of the imide fragments in **16–18** are the same as in the corresponding arylalkyl imides (**10 α** , **11** and **15**) having no *ortho*-hydroxyl groups. The addition of the hydroxyl group dramatically changes the structures of the hydrogen bond aggregates, however. In **16**, the anticipated eight-membered ring dimer of **10 α** is disrupted by the additional hydroxyl group, which hydrogen bonds to the imide NH. This same NH...O(H) interaction in **18** disrupts the anticipated hydrogen bond chain that is observed in **15**. In **17**, however, the additional OH proton donor is accommodated most efficiently by simply bonding to the otherwise unused benzoyl oxygen.

DISCUSSION

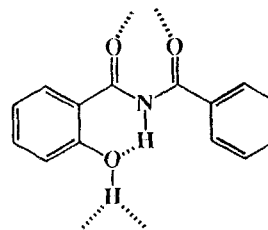
Conformational preferences, hydrogen bonding interactions and crystal packing forces play key roles in determining the patterns of the solid-state aggregates of acyclic imides. In the absence of hydrogen bonding interactions or packing considerations, we might expect to see imides in the stable *cis-trans* conformation, which has a lower dipole moment and predominates in solution for all analogs except **9**.¹⁷ In concentrated solutions and in the solid state, *cis-trans* imides form eight-membered ring hydrogen bond dimers (A). This aggregate is stabilized by strong two-centered hydrogen bonds from the NH of one molecule to the *cis* carbonyl group of the other in the dimer pair, but is destabilized by not using the *trans* carbonyl group in hydrogen bonding.



16

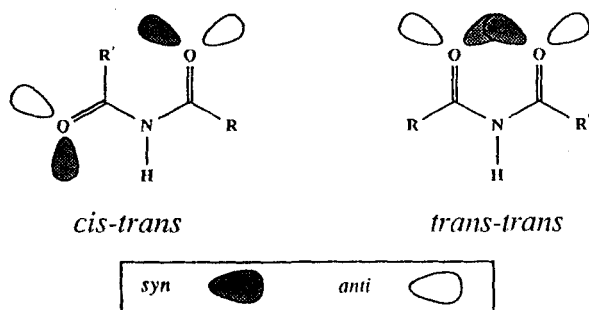


17



18

In the solid state, where intermolecular hydrogen bonding interactions and crystal packing forces become important, the imides occur predominantly in the *trans-trans* conformation. Imides adopting this conformation form chains linked by either three-centered (B) or two-centered (C) hydrogen bonds. A common feature of all three hydrogen bond aggregates is that only the *syn* lone pairs of electrons are used in hydrogen bonding. Of the *syn* lone pairs, only those on the *trans* carbonyl oxygens of *cis-trans* imides are not used in hydrogen bonding.



Acyclic imides not only form predictable aggregate structures, but these aggregates have been found to pack in predictable patterns themselves. Imides in A-type hydrogen bonding patterns are most frequently found in sheets, while B- or C-type chains pack closely in columns.

How conformational preferences, hydrogen bonding interactions and crystal packing contribute to the stabilization of specific solid-state aggregates is determined primarily by the nature of the R and R' groups. The conformational preferences of the arylalkyl imides, for example, can be understood from analysis of the steric requirements of their R and R' groups. In **10a**, **11** and **12**, the primary alkyl groups are not sterically demanding, so the *cis-trans* conformation is found. Increasing the bulk of the alkyl groups destabilizes the *cis-trans* form relative to the *trans-trans* conformation, so the latter is observed in all arylalkyl imides (**13**–**15**) substituted with secondary, tertiary or phenyl groups. The occurrence of two conformers of **10** (R = Me) has been explained in terms of the similar conformational energies for the two forms.

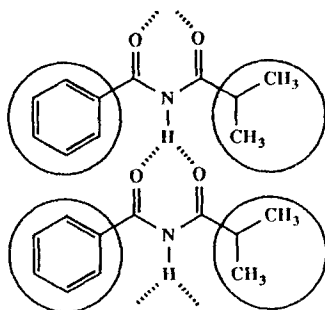
Rationalizing the formation of specific aggregates based on the steric requirements of the R groups alone represents an oversimplification of what is occurring in the solid state, however. For example, steric considerations cannot be used to explain the conformational preferences and occurrence of B-type hydrogen bonding patterns of the diacylamines **1b** and **2**–**4** (Table 4). In these imides, both R groups are primary and therefore not sterically demanding, so the *cis-trans* conformation would be expected. By forcing imides clearly preferring

the *cis-trans* conformation into the *trans-trans* form, the three-centered hydrogen bonds in aggregate B apparently stabilize imides to a greater extent than does one strong, two-centered hydrogen bond to a single carbonyl group, leaving the other group free, as in aggregate A.

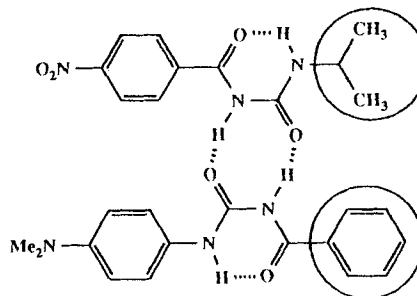
If B-type aggregates are observed when the R groups are small, and increasing the size of the substituents only serves to stabilize the *trans-trans* conformer relative to the *cis-trans* form, the imides should always be *trans-trans* in the solid state. Other arguments, such as crystal packing, are therefore needed to explain the formation of *cis-trans* imide dimers (A) in the solid state. The B-type aggregates are observed for imides bearing large and small substituents, but only when R and R' are of comparable shape and size. When the substituents have significantly different spatial requirements, the A- or C-type aggregates form preferentially. This relationship between R group compatibility and preferential aggregation suggests that the bifurcated hydrogen bond chains form the highest density structures when the R groups are comparable in shape and size. Alternatively, when the spatial requirements of the substituents are mismatched, the A- or C-type aggregates are observed because they close pack more efficiently. Other packing forces, such as dipolar interactions, may also be influencing the aggregate patterns. With the limited data set, however, it is very difficult to assess the role of these interactions in the overall packing of the imides. We have previously observed in **1b** and **2**–**4** that the stabilization provided by specific hydrogen bonding interactions can override imide conformational preferences. We now find that packing effects may preclude the formation of the most stable B-type hydrogen bond aggregates.

Since bifurcated hydrogen bond chains are observed only when the R groups are comparable in shape and size, the formation of this aggregate pattern in **13** may serve as an indication that isopropyl and phenyl groups are isosteric. The similar spatial requirements of isopropyl and phenyl groups have been previously observed in the elegant studies carried out by Endo, whereby the acylurea framework was used to evaluate the role of shape similarity in molecular recognition.¹⁸ Endo found that crystalline 1:1 complexes of substituted acyclic acylureas, including the complex of 1-isopropyl-3-(*p*-nitrobenzoyl)urea and 1-(*p*-dimethylaminophenyl)-3-phenylurea (see formula), can be formed provided that the shapes of the R groups are comparable.¹⁹

The compatibility of these R groups in acyclic imides is evident when comparing **5**, **13** and **15**, the only imides to form bifurcated hydrogen bond chains and to crystallize in polar space groups (all other imides in this study forming the B-type aggregate are in centric space groups). The hydrogen bond chains in **5**, **13** and **15** are all oriented along the *c* axis [Figures 2(a)–(c)], and the



13



acylureas

molecules pack in layers. The c axes of these analogs are similar ($c = 8.876, 9.009$ and 9.001 Å in **5**, **13** and **15**, respectively), indicating that the isopropyl and phenyl groups have at least one dimension in common, and the groups orient so their common dimensions are parallel to the chain direction.

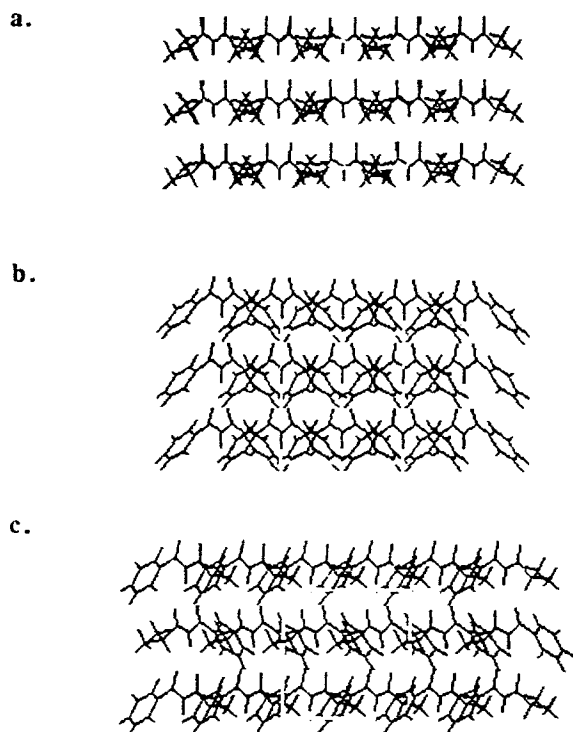
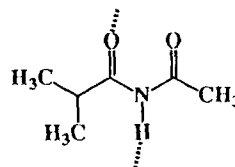


Figure 2. Bifurcated hydrogen bond chains of (a) **5**, (b) **15** and (c) **13**. These imides crystallize in polar space groups, with the chains formed along the c axes and oriented parallel to one another. The chains pack with the imides in layers in these structures. The repeat units are all equally spaced as evident by the very similar unit cell lengths along the chains ($c = 8.876, 9.009$ and 9.001 Å in **5**, **13** and **15**, respectively)

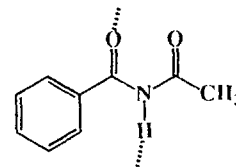
The packing of the hydrogen bond chains of **5**, **13** and **15** in the a and b directions is shown (Figure 3), from which the spatial requirements of the substituents in these directions are seen. In diisobutyramide, **5**, the isopropyl groups in the neighboring chains appear to be pointing at one another [Figure 3(a)]. The phenyl groups in **15**, on the other hand, prefer to be in the grooves of the neighboring chains [Figure 3(b)]. When these groups are present in the same molecule, as in **13**, the phenyl and isopropyl substituents partition themselves [Figure 3(c)], so that the phenyl groups are only interacting with phenyl groups and the isopropyl groups are only seeing other isopropyl groups. In this structure, the phenyl groups in the grooves formed by neighboring chains and the isopropyl groups appear to be interacting head on, just as they do in **5** and **15**.

The arrangement of the isopropyl and phenyl groups in **13** suggests that these substituents are isosteric since the groups pack as if they and their partners were the same. Despite the similar spatial requirements of the substituents, there is no disorder in this structure. This finding is not surprising since isopropyl and phenyl groups are not isoelectronic. Clearly the attractive dispersive forces of the isopropyl groups and the dipolar interactions between phenyl groups dictate that these substituents will be partitioned in **13**.

The similarity between the packing of isopropyl and phenyl substituents is also revealed in **6** and **10β**, the only imides to form the anomalous C-type aggregates shown. The hydrogen bond aggregates of these analogs are identical, presumably because each analog has a methyl group as one of its substituents and the other groups (phenyl and isopropyl) are comparable in shape



6



10β

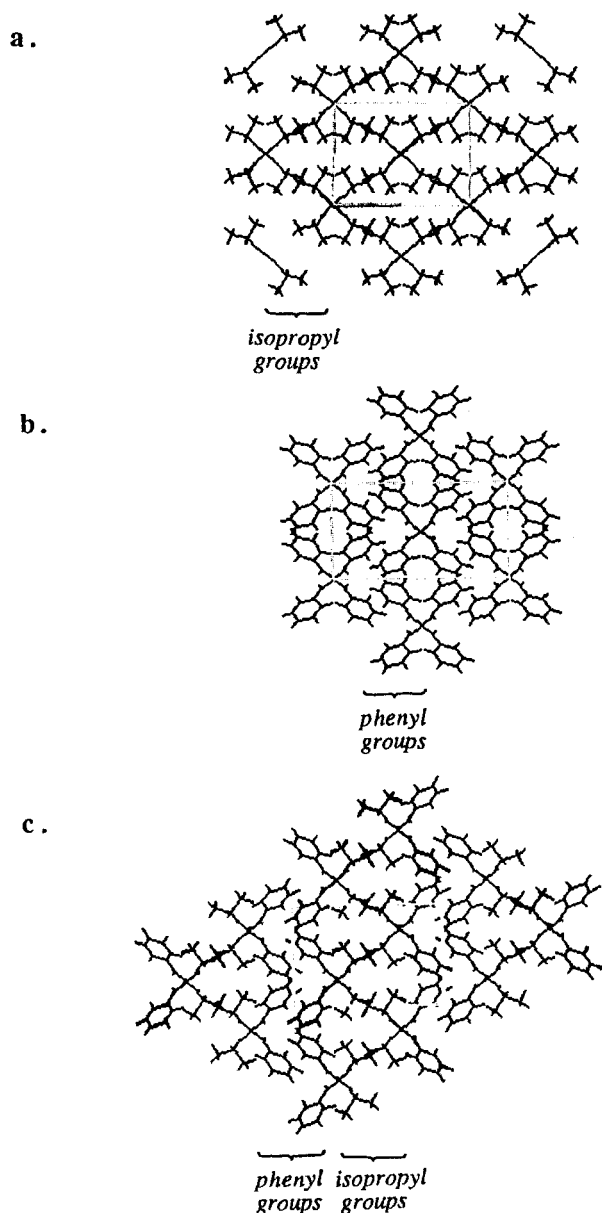


Figure 3. Crystal packing of the bifurcated hydrogen bond chains of (a) **5**, (b) **15** and (c) **13** as seen along the chain axes. The isopropyl groups in neighboring chains appear to be pointing toward one another in (a). The phenyl groups in (b) prefer to position themselves in the grooves of the neighboring imide chains. In (c), the phenyl and isopropyl groups of **13** partition themselves. Both the isopropyl and phenyl regions in **13** are identical with the corresponding regions of **5** and **15**, with the isopropyl groups directed at one another and the phenyl groups in the grooves of neighboring chains. The arrangement of the isopropyl and phenyl groups in **13** indicates that these groups are isosteric (as in **5** and **15**)

and size. It is reasonable to expect that a B-type aggregate should not form in **6** or **10 β** since the two R groups are significantly different in size, thus preventing the bifurcated hydrogen bond chains from close packing efficiently. What is unexpected in these structures is that the less stable *trans-trans* conformation is present even though it is not stabilized by bifurcated hydrogen bonding interactions. In **10**, the conformational energies of the *cis-trans* and *trans-trans* forms (columns 3 and 4, Table 3) are similar, so it is not unreasonable to find the only slightly less favorable conformation in the solid state.

From the previous analyses, diacetamide, **1 α** , can be viewed as an anomaly since both R and R' are small, and packing of *trans-trans* chains should not be problematic. That **1 α** is the stable form of this imide again indicates that packing influences are as important as conformational preferences or hydrogen bonding interactions in determining the structures of the solid-state molecular aggregates.

CONCLUSIONS

We have demonstrated in our systematic studies of the molecular recognition properties of acyclic imides that it is possible to determine how crystal packing forces, hydrogen bonding and conformational preferences balance one another in forming specific hydrogen bonding patterns. The size and shape of the R and R' groups seem to play a major role in determining how acyclic imides prefer to aggregate. Certain features are common to the nine crystal structures (**1 α** , **1 β** , **3**, **9**, **10 β** , **11-13** and **15**) from the literature, the crystal structure (**5**) presented in this paper and the five other solid-state aggregates of simple (no additional hydrogen bonding substituents) acyclic imides that have been characterized spectroscopically:

1. The NH protons and at least one carbonyl oxygen are used in hydrogen bonding.
2. Only the *syn* lone pairs of electrons of the carbonyl groups are used in hydrogen bonding.
3. *Cis-trans* imides (three crystal structures) pack in A-type hydrogen bond patterns.
4. *Trans-trans* imides (five crystal structures) usually form B-type hydrogen bond chains, but C-type aggregates (one crystal structure) are also possible.
5. When the R and R' substituents are comparable in shape and size, B-type aggregates are observed. When they have significantly different spatial requirements, A- and C-type aggregates form.

These correlations should be useful for predicting *a priori* which of several possible hydrogen bond patterns will form for new acyclic imides in the solid state.

ACKNOWLEDGMENTS

We are grateful to Professor Doyle Britton and Chris Blaine, Department of Chemistry, University of Minnesota, for crystallographic assistance and NIH (GM 42148-01) for financial support.

REFERENCES

1. (a) J. Rebek, Jr, *Pure Appl. Chem.* **61**, 1517–1522 (1989); (b) J. Rebek, Jr, *Science* **235**, 1478–1484 (1987); (c) J. Rebek, Jr, *Acc. Chem. Res.* **23**, 399–404 (1990); (d) S.-K. Chang and A. D. Hamilton, *J. Am. Chem. Soc.* **110**, 1318–1319 (1988); (e) A. Echavarren, A. Galán, J.-M. Lehn and J. de Mendoza, *J. Am. Chem. Soc.* **111**, 4994–4995 (1989).
2. A. D. Hamilton and D. Little, *J. Chem. Soc., Chem. Commun.* 297–300 (1990).
3. (a) M. C. Etter, D. L. Parker, S. R. Ruberu, T. W. Panunto and D. Britton, *J. Inclus. Phenom. Mol. Recogn. Chem.* **8**, 395–407 (1990); (b) M. C. Etter, G. M. Frankenbach and D. A. Adsmond, *Mol. Cryst. Liq. Cryst.* **187**, 25–39 (1990); (c) T. W. Panunto, Z. Urbánczyk-Lipkowska, R. Johnson and M. C. Etter, *J. Am. Chem. Soc.* **109**, 7786–7797 (1987); (d) M. C. Etter and G. M. Frankenbach, *Chem. Mater.* **1**, 10–12 (1989).
4. M. C. Etter and S. M. Reutzel, *J. Am. Chem. Soc.* **113**, 2586–2598 (1991).
5. (a) K. Vyas, V. M. Rao and H. Manohar, *Acta Crystallogr., Sect. C* **43**, 1201–1204 (1987); (b) J. McConnan and A. W. Titherley, *J. Chem. Soc.* **89**, 1319–1339 (1906).
6. (a) T. Uno and K. Machida, *Bull. Chem. Soc. Jpn* **34**, 551–556 (1961). (b) K. Baburao, A. M. Costello, R. C. Petterson and G. E. Sander, *J. Chem. Soc. (c)* 2779–2781 (1968).
7. *Supplementary material: structure factors, positional parameters, anisotropic thermal parameters and intra- and intermolecular bond lengths and angles*, 13 pp. Available on request from the authors.
8. C. J. Gilmore, *J. Appl. Crystallogr.* **17**, 42–46 (1984).
9. P. T. Beurskens, *Technical Report*, University of Nijmegen, Vol. 1 (1984).
10. M. C. Etter, J. C. MacDonald and J. Bernstein, *Acta Crystallogr., Sect. B* **46**, 256–262 (1990).
11. *Macromodel*, Department of Chemistry, Columbia University, New York, January 1988 update, Version 2.0 (Vax).
12. (a) S. J. Weiner, P. Kollman, D. A. Case, U. Singh, C. Ghio, G. Alagaona, S. Profeta, Jr, and P. Weiner, *J. Am. Chem. Soc.* **106**, 765–784 (1984); (b) S. J. Weiner, P. A. Kollman, D. T. Nguyen and D. A. Case, *J. Comput. Chem.* **7**, 230–252 (1986).
13. M. C. Etter and S. M. Reutzel, in press.
14. (a) P. M. Matias, G. A. Jeffrey and J. R. Ruble, *Acta Crystallogr., Sect. B* **44**, 516–522 (1988); (b) Y. Kuroda, Z. Taira, T. Uno and K. Osaki, *Cryst. Struct. Commun.* **4**, 321–324 (1975); (c) T. Uechi, T. Watanabe and K. Osaki, *Sci. Rep. Osaka Univ.* **15**, 1–12 (1966); (d) J. Hvosllef, M. L. Tracy and C. P. Nash, *Acta Crystallogr., Sect. C* **42**, 353–360 (1986); (e) R. B. Bates, K. D. Janda and M. E. Wright, *Acta Crystallogr., Sect. C* **41**, 263–264 (1985).
15. V. Mizrahi and M. L. Niven, *S. Afr. J. Chem.* **36**, 137–142 (1983).
16. K. Vyas and H. Manohar, *Mol. Cryst. Liq. Cryst.* **137**, 37–43 (1986).
17. E. A. Noe and M. Raban, *J. Am. Chem. Soc.* **97**, 5811–5820 (1975).
18. T. Endo, *Top. Curr. Chem.* 91–111 (1984).
19. T. Endo, K. Miyazawa, M. Endo, A. Uchida, Y. Ohashi and Y. Sasada, *Chem. Lett.* 1989–1992 (1982).